

Exp.-Nr. A2-7/05  
Eingang: 26.08.05  
an PAC:

## Mainz Microtron MAMI

**Collaboration A2:** "Real Photon Experiments"

Spokesperson: A. Thomas

### Proposal for an Experiment

**"Helicity Dependence of Meson Photoproduction on the Proton"**

#### Collaborators :

Crystal Ball @ MAMI and TAPS collaborations

#### Contact Persons :

H.-J. Arends, Institut für Kernphysik, Universität Mainz  
A. Braghieri, INFN-Sezione di Pavia, Pavia, Italy  
M. Kotulla, II. Physikalisches Institut, Universität Giessen  
A. Thomas, Institut für Kernphysik, Universität Mainz

#### Abstract of Physics :

We propose to perform a precise measurement of the helicity asymmetries of  $\pi^0$ ,  $\pi^0\pi^0$ ,  $\pi^0\pi^+$ , and  $\eta$  production at photon energies in the region of the  $D_{13}(1520)$ - and  $F_{15}(1680)$  resonances in order to determine their helicity amplitudes and the contribution of these reaction channels to the GDH integrand.

#### Abstract of Equipment :

We require a beam of tagged, circularly polarized photons incident on a longitudinally polarized target and the  $4\pi$  Crystal Ball photon spectrometer in combination with TAPS as forward wall and a Čerenkov detector for suppression of electromagnetic background. The upgraded Glasgow tagging system will provide the tagged, polarized photon beam.

#### MAMI-Specifications :

beam energy	855 and 1500 MeV
beam current	< 100 nA
time structure	cw
polarization	circularly polarized photons

#### Experiment-Specifications :

experimental hall/beam	A2
detector	Crystal Ball and TAPS as forward wall
target	polarized Butanol

#### Beam-Time Request :

set-up without beam	8 weeks
set-up/tests with beam	24 hours
data taking	250 hours at 855 MeV
data taking	250 hours at 1500 MeV
target re-polarization	150 hours
data taking	200 hours at 1500 MeV with liq. hydrogen target (in conjunction with other experiments)

# Helicity Dependence of Meson Photoproduction

## Abstract

We propose to measure the helicity asymmetry of meson photoproduction with neutral final states using the Crystal Ball/TAPS setup together with the new Mainz frozen-spin target and the circularly polarized photon beam at MAMI C. Single  $\pi^0$  production reveals a strong sensitivity to the  $D_{13}(1520)$ - and  $F_{15}(1680)$  resonances,  $\eta$  production will allow to investigate the contribution of  $P_{11}(1710)$ ,  $S_{11}(1650)$ , and  $F_{15}(1680)$  resonances. The helicity asymmetry and helicity dependent invariant mass distributions in double  $\pi^0$  and  $\pi^+\pi^0$  production will help to pin down resonance contributions in the intermediate states and to clarify the dominant reaction mechanisms. The contribution of these reaction channels to the GDH integrand will be determined.

## 1 Motivation

The helicity asymmetry of the total photoabsorption cross section using circularly polarized photons and longitudinally polarized nucleon gives access to the investigation of the Gerasimov-Drell-Hearn (GDH) sum rule [1], which connects the static properties of the nucleon (e.g. mass, anomalous magnetic moment) with the dynamics of the excitation spectrum. The current situation up to photon energies of about 1.6 GeV is shown in fig. 1. According to MAID[2], single pion production is the dominant contribution in the  $\Delta$ -region and third resonance region, whereas in the second resonance region, double pion production plays an important role. This is even more puzzling, as for the neutron [3] the situation seems to be completely different, see fig. 2. While the proton and neutron data tend to be similar, the one-pion part of MAID shows a pronounced difference. This clearly shows that the contributing reaction channels to the GDH sum rule have to be studied in more detail in order to get a better understanding of the helicity structure of the nucleon.

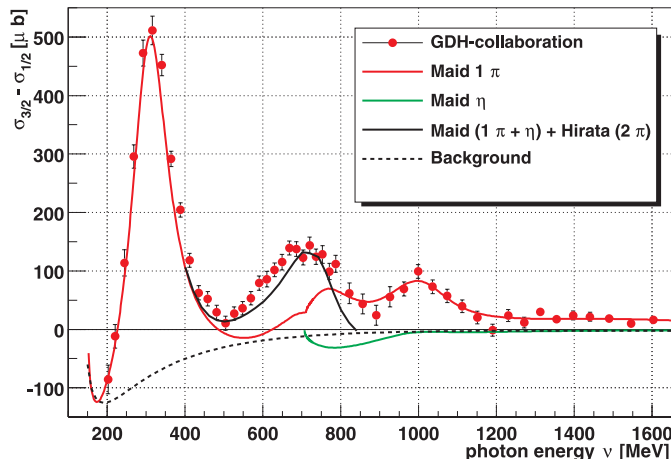


Figure 1: The measured helicity difference of the total cross section compared to theoretical analyses.

Moreover, the helicity asymmetry of partial reaction channels has proven to be a new and sensitive observable which can be used to improve our knowledge on the helicity amplitudes of nucleon resonances and can help to disentangle the reaction mechanisms in particular reaction channels such as double pion photoproduction. In the first round of the GDH-experiments at MAMI the region of the  $\Delta(1232)$  and the  $D_{13}(1520)$  resonances has been explored. Since the  $\Delta$  has been studied extensively over many decades and a huge number of high quality cross

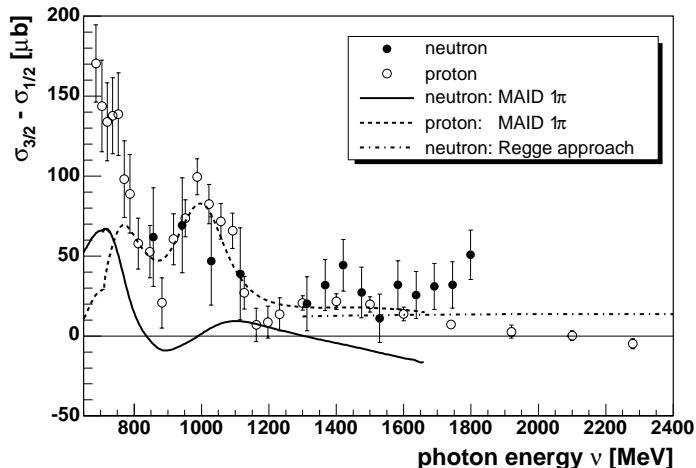


Figure 2: The measured helicity difference of total cross sections on the proton (open circles) and neutron (solid circles) compared to MAID [2]. (Figure from ref. [3]).

section and single polarization data is available, one cannot expect to find any surprises here when looking at the double polarization observables. However, it can be taken as a confirmation, that the E2/M1 ratio of the  $N \rightarrow \Delta$  transition obtained from the helicity observables is fully consistent with the results from other methods. The full data set from the GDH-experiment in the  $\Delta$ -region is contained in Ref. [4].

### 1.1 Single Pion Production in the $D_{13}(1520)$ -Region

At higher energies around the region of the second resonances where the resonance properties are known much less, we can expect to gain new information. The helicity difference reveals a high sensitivity to the  $D_{13}(1520)$ -resonance. The multipoles  $E_{2-}$  and  $M_{2-}$  (E1 and M2 transitions, respectively) are related to the helicity amplitudes in the following way:

$$A_{1/2}(D_{13}) \sim E_{2-} - 3M_{2-}, \quad A_{3/2}(D_{13}) \sim \sqrt{3}(E_{2-} + M_{2-}).$$

The recent results of Ref. [5] on  $\pi^0$  production are shown in fig. 3. At lower photon energies, the data are in a good agreement with the model predictions, but there is a clear systematic discrepancy when the  $D_{13}(1520)$  resonance is approached. In order to extract information about this resonance, a fit of our unpolarized and polarized differential cross sections, based on MAID [2], has been performed (see dotted curve). The results for the helicity amplitudes are  $A_{1/2} = -38 \pm 3$  and  $A_{3/2} = 147 \pm 10$ , all in units of  $10^{-3} \text{ GeV}^{-1/2}$ . This is a significant change with respect to the values listed by the Particle Data Group [7] ( $A_{3/2} = 166 \pm 5$ ,  $A_{1/2} = -24 \pm 9$ ). Expressed in terms of the CGLN multipoles, the ratio  $M_{2-}/E_{2-}$  has increased from 0.45 to 0.56.

In a similar way the single- $\pi^+$  production was investigated in the second resonance region. Preliminary data on the total unpolarized and polarized cross section are shown in Fig. 4 in comparison with the results of MAID and SAID. The differences of the two analyses are much more pronounced in the polarized case. This originates from significant differences in the balance of the  $E_{0+}$  and  $E_{2-}$  multipoles, which result in the same sum in the unpolarized case but enter with opposite signs in  $\Delta\sigma$ .

While these first measurements clearly showed the potential of this observable, the data are still limited in statistical accuracy and in the photon energy range covered. The maximum energy of MAMI B allowed to cover only approximately the lower half of the  $D_{13}(1520)$ -resonance.

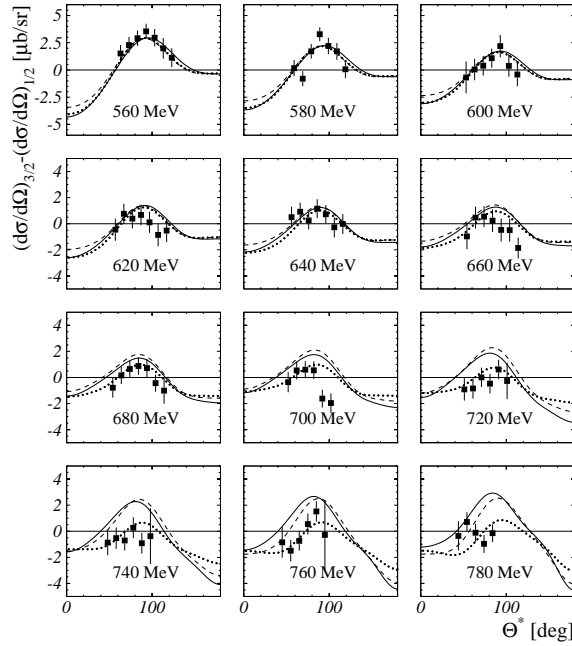


Figure 3: The measured helicity dependent differential cross section  $\Delta_{31}$  for  $\vec{\gamma}\vec{p} \rightarrow p\pi^0$  (solid squares) compared to the multipole analyses SAID [6] (solid curve) and MAID [2] (dashed curve). The dotted curve represents the modified solution of MAID. The errors shown are statistical only.

## 1.2 Single Pion Production in the $F_{15}(1680)$ -Region

At higher energies up to about 1.5 GeV the  $F_{15}(1680)$  can be studied in a similar way. The sensitivity of the helicity observable E was investigated using MAID2003 [2]. The results are shown in fig. 5 for two cms-angles of the  $\pi^0$  as a function of the photon energy. As can be clearly seen, there is a significant sensitivity to the  $F_{15}(1680)$  in the energy range of 1000-1400 MeV.

An overview of the current values of the helicity amplitudes in the second and third resonance region from various analyses is given in table 1.

Table 1: Helicity amplitudes  $A_{1/2}$  and  $A_{3/2}$  for proton resonances in the second and third resonance region from various analyses.

		PDG	VPI95	GW02	MAID98	Maid02	Maid03
$P_{11}(1440)$	$A_{1/2}$	$-65 \pm 4$	$-63 \pm 4$	$-67 \pm 4$	-71	-78	-77
$S_{11}(1535)$	$A_{1/2}$	$90 \pm 30$	$60 \pm 4$	$30 \pm 4$	67	79	73
$D_{13}(1520)$	$A_{1/2}$	$-24 \pm 9$	$-20 \pm 4$	$-24 \pm 4$	-17	-23	-30
	$A_{3/2}$	$166 \pm 5$	$167 \pm 4$	$135 \pm 4$	167	169	166
$S_{11}(1650)$	$A_{1/2}$	$53 \pm 16$	$69 \pm 4$	$74 \pm 4$	39	31	32
$F_{15}(1680)$	$A_{1/2}$	$-15 \pm 6$	$-10 \pm 4$	$-13 \pm 4$	-10	-17	-24
	$A_{3/2}$	$133 \pm 12$	$145 \pm 4$	$129 \pm 4$	138	143	134
$D_{33}(1700)$	$A_{1/2}$	$104 \pm 15$	$90 \pm 4$	$89 \pm 4$	86	147	135
	$A_{3/2}$	$85 \pm 22$	$97 \pm 4$	$92 \pm 4$	85	199	213

We propose to improve our previous results on the  $D_{13}(1520)$  resonance and extend this investigation to the  $F_{15}(1680)$ , using single  $\pi^0$  and  $\pi^+$  photoproduction.

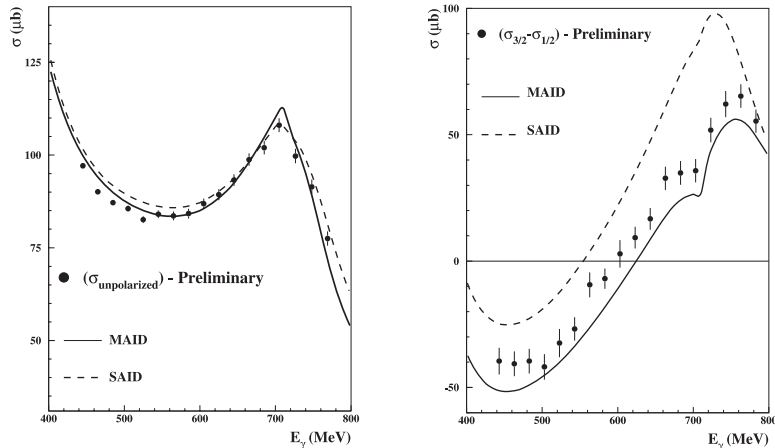


Figure 4: The preliminary total cross section (left) and helicity difference  $\Delta\sigma = \sigma_{3/2} - \sigma_{1/2}$  (right) for the reaction  $\vec{\gamma}\vec{p} \rightarrow n\pi^+$  in comparison with results from MAID and SAID.

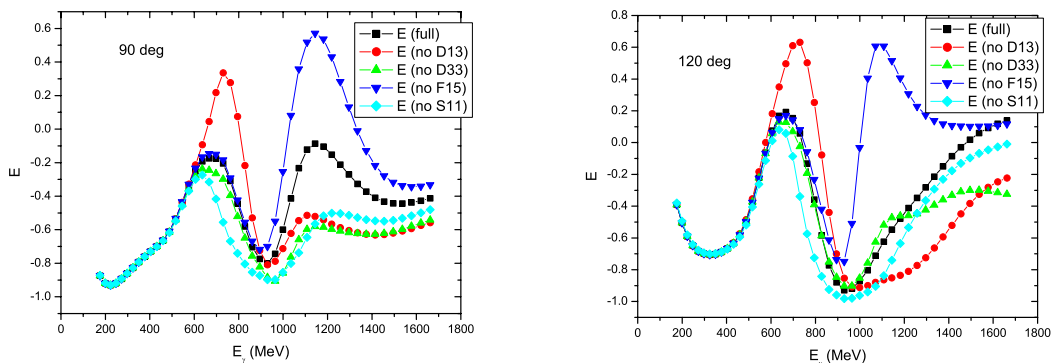


Figure 5: The helicity asymmetry  $E$  for the reaction  $\vec{\gamma}\vec{p} \rightarrow p\pi^0$  at 60 deg. (left) and 120 deg. (right) studied with MAID2003 by switching off individual resonances.

### 1.3 $\eta$ -production

It is well known that the  $S_{11}(1535)$  appears as a resonance in the multipole  $E_{0+}$  ( $E1$ ) just above  $\eta$  threshold and dominates the  $\eta$  photoproduction process at energies close to threshold. Since the  $S_{11}$  is a pure helicity-1/2 resonance this means that one expects the helicity asymmetry to be  $E \approx 1$ , as was also confirmed by the GDH-experiment [8]. This can serve as a calibration reaction for the product of beam and target polarizations.

At higher energies, however, the situation changes, and a significant sensitivity to higher resonances occurs, mainly to  $P_{11}(1710)$ ,  $S_{11}(1650)$ , and  $F_{15}(1680)$ . This is clearly visible in fig. 6, where the results from an eta-MAID [9] calculation are shown as function of the photon energy. Fig. 7 shows the angular distributions at  $E_\gamma=1150$  MeV both for the differential cross section and the helicity asymmetry. A wealth of structure appears in the angular distribution of the helicity asymmetry, which will help to disentangle the influence of the individual resonances.

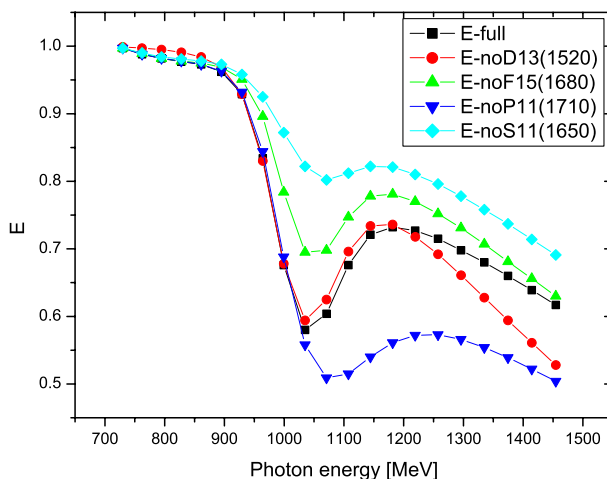


Figure 6: The helicity asymmetry from eta-MAID [9] for the reaction  $\vec{\gamma}\vec{p} \rightarrow p\eta$ .

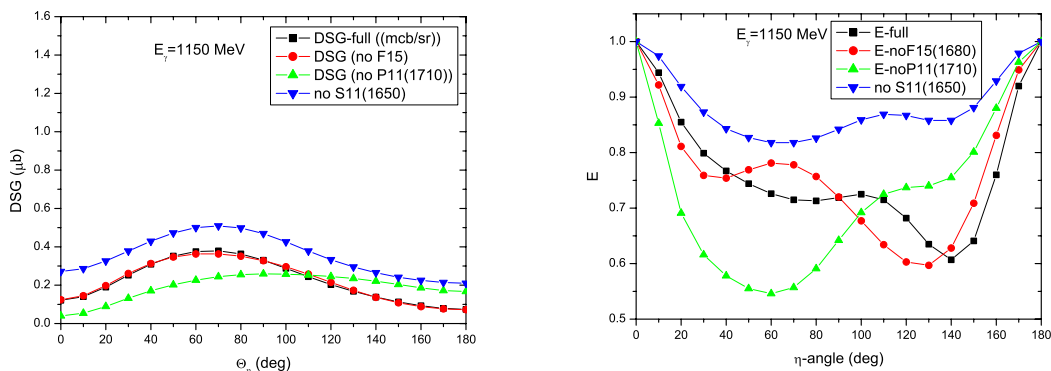


Figure 7: Differential cross section (left) and helicity asymmetry  $E$  (right) for the reaction  $\vec{\gamma}\vec{p} \rightarrow p\eta$  at a photon energy of 1150 MeV studied with eta-MAID by switching off individual resonances.

## 1.4 Double Pion Production

The main issue in double pion production is to clarify the dominant reaction mechanisms. The fact, that higher resonances tend to have a higher branching ratio to  $\pi\pi N$  than to  $\pi N$  final states, makes this reaction also attractive in order to investigate their photon couplings via double pion production. This, however, requires the development of partial wave analyses, as it is in progress by the Bonn group [10].

The double pion production channels  $n\pi^+\pi^0$ ,  $p\pi^+\pi^-$ , and  $p\pi^0\pi^0$  were separately analyzed in the GDH-experiment at MAMI. As a first example we show in Fig. 8 the helicity-dependent cross section for  $\vec{\gamma}\vec{p} \rightarrow n\pi^+\pi^0$  [18]. It is evident that the present models can only describe the data in a semi-quantitative way.

Fig. 8 shows very nicely a peaking of the cross sections around the position of the  $D_{13}(1520)$  resonance. A previous TAPS experiment [15] attributed a significant strength of the  $\gamma p \rightarrow n\pi^+\pi^0$  channel to the decay of the  $D_{13}(1520)$  via the  $\rho$  meson into the nucleon ground state. The strength of the  $\rho$  contribution was deduced from the comparison of the simultaneously measured invariant mass distributions of the  $\pi^0\pi^0$  and  $\pi^+\pi^0$  systems. Our proposed experiment could

improve on these findings in several points. The helicity dependent invariant mass distributions for the  $n\pi^+\pi^0$  channel will provide a powerful tool to assign the  $\rho$  strength to a particular resonance like the  $D_{13}(1520)$  or other reaction processes. Moreover, the limitation in the beam energy of the previous experiments will be overcome allowing to study the full range of the second resonance region and higher resonances. The  $\rho$ - $D_{13}(1520)$  coupling is of vital interest since the non-observation of the second resonance region in the total photo-absorption cross section on nuclei has often been attributed to the broadening of the  $D_{13}(1520)$  resonance [16]. Such a broadening could arise from a coupling of the resonance to the  $N\rho$  final state since the  $\rho$  meson itself is appreciably broadened in the nuclear medium [17].

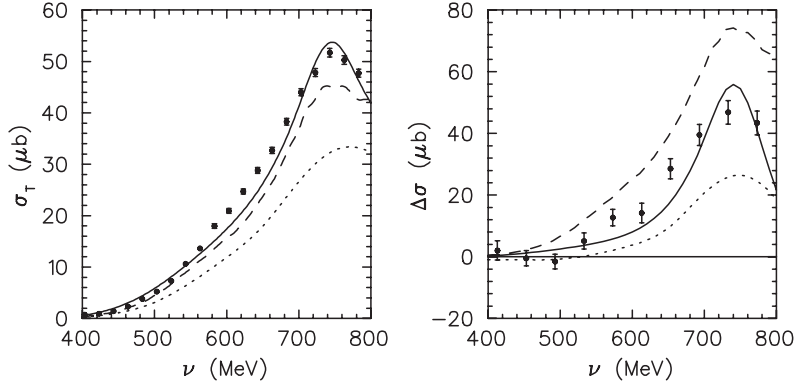


Figure 8: The total cross section  $\sigma_T$  and the helicity difference  $\Delta\sigma = \sigma_{3/2} - \sigma_{1/2}$  for the reaction  $\vec{\gamma}\vec{p} \rightarrow n\pi^+\pi^0$ . The theoretical predictions are given by the solid lines [13], dashed lines [11], and dotted lines [14]. The data are from MAMI [18].

For the  $p\pi^+\pi^-$  reaction, the helicity-3/2 part shows a resonant behaviour, whereas  $\sigma_{1/2}$  is a smoothly rising function of the photon energy. This reaction peaks at about 650 MeV, definitely below the positions of the  $D_{13}(1520)$  and  $S_{11}(1535)$  resonances. This again is an experimental indication that two-pion production can not be simply explained by a resonance driven s-channel mechanism, corroborating the statement made above on the complicated nature of the reaction mechanisms.

The  $p\pi^0\pi^0$  final state is of particular interest because of its high sensitivity to the resonance contributions. In this case, the intermediate  $\Delta\pi$  excitation term is in fact strongly suppressed with respect to the  $n\pi^+\pi^0$  and  $p\pi^+\pi^-$  reactions and, due to isospin conservation, no intermediate  $\rho$ -contribution is possible. Total cross sections were measured by TAPS and DAPHNE at MAMI and by GRAAL [19], see figure 9.

There are two models that reproduce equally well the total  $p\pi^0\pi^0$  cross section up to about 800 MeV although with completely different interpretations. The Valencia model [11] predicts the dominance of the intermediate  $D_{13}(1520)$  excitation with subsequent  $D_{13}(1520) \rightarrow \Delta^+\pi^0$  and  $\Delta^+ \rightarrow p\pi^0$  decays.

In contrast the Murphy-Laget model [12] which extends up to photon energies of 1.5 GeV predicts a dominant excitation of the  $P_{11}(1440)$  resonance followed by  $P_{11}(1440) \rightarrow p\sigma$  and  $\sigma \rightarrow \pi^0\pi^0$  decays, where  $\sigma$  represents a correlated pair of pions in a relative s-wave. The second peak in the cross section at about 1100 MeV, seen by GRAAL is explained by the same mechanism based on the  $P_{11}(1710)$  resonance.

Our data shows that  $\sigma_{3/2}$  clearly dominates  $\sigma_{1/2}$  and peaks at about 700 MeV, see Fig. 10. According to both models, the  $D_{13}(1520)$  resonance is largely responsible for the observed dominance of  $\sigma_{3/2}$ , via the process  $\gamma N \rightarrow D_{13}(1520) \rightarrow \pi\Delta \rightarrow \pi\pi N$ . However, the non-negligible  $\sigma_{1/2}$  cross section points to significant non-resonant effects and to mechanisms involving the intermediate excitation of additional spin-1/2 resonances, such as  $P_{11}(1440)$  or  $S_{11}(1535)$ .

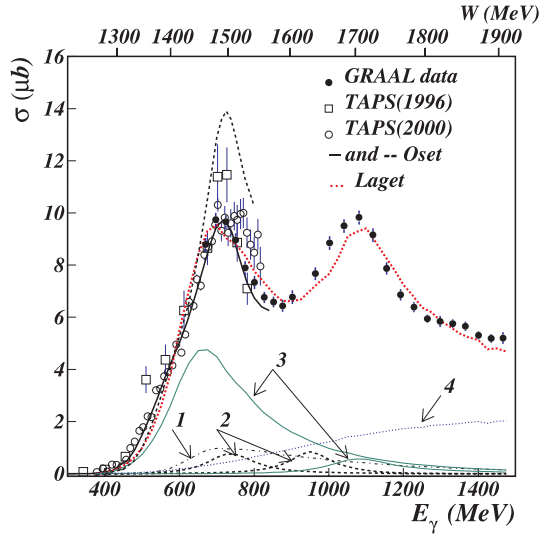


Figure 9: Total cross section for the reaction  $\vec{\gamma}\vec{p} \rightarrow p\pi^0\pi^0$ , from ref. [19] with theoretical predictions from Oset et al. [11] and Murphy-Laget [12].

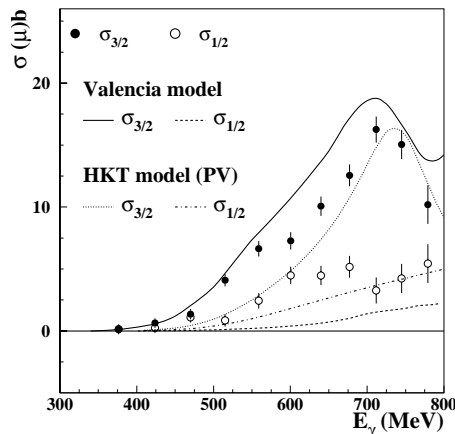


Figure 10: Preliminary helicity dependent cross sections  $\sigma_{3/2}$  and  $\sigma_{1/2}$  for the reaction  $\vec{\gamma}\vec{p} \rightarrow p\pi^0\pi^0$  from MAMI [20]. The theoretical predictions are from the Valencia[11] and HKT[13] models.

Hirata et al. [13](HKT) investigate effects of non-resonant photoproduction. From comparing their results to the total unpolarized cross section they conclude that the pseudoscalar  $\pi NN$  coupling (PS) is preferable over the pseudovector coupling. However, the helicity-dependent data are described better by assuming pseudovector coupling (PV).

Recently, also the Mainz group of Arenhövel et al. has done calculations of double pion production including double polarization observables [21].

We plan to measure the helicity asymmetry of double  $\pi^0$  production from threshold up to 1400 MeV over a wide angular range. Compared to our existing data a very important additional feature will be the capability to study invariant mass distributions for the helicity states separately. This is essential to further pin down resonance contributions in the intermediate states and to clarify the dominant reaction mechanisms.

In addition, as mentioned in the beginning, a crucial question is the contribution of the double pion production channels to the GDH-integrand in the region of the third resonances, see figs. 1 and 2, which can be clarified with this measurement.



## 2 Experimental setup

The previous GDH experiments at MAMI were carried out with the detector DAPHNE, which was well suited for the detection of charged particles in the final state. The response for neutral particles, however, was limited. In particular, the energies of the emission angles of  $\pi^0$  and  $\eta$  mesons could not be measured and invariant mass distributions could not be obtained. Therefore, the Crystal Ball with the TAPS forward wall is an ideal detector to extend the previous experiments to neutral channels.

The experiment will be carried out at the tagged photon facility of the MAMI accelerator in Mainz. Circularly polarized electrons are produced by bremsstrahlung of longitudinally polarized electrons. The source of polarized electrons, based on the photoeffect on strained GaAs crystals, delivers routinely electrons with a degree of polarization of about 75% or higher. Photons with a degree of polarization of more than 60% of the electron polarization are obtained in the upper half of the energy spectrum.

Polarized nucleons will be available in the new Mainz frozen spin target that is presently under construction and is expected to be operational in early 2007. The system consists of a hori-

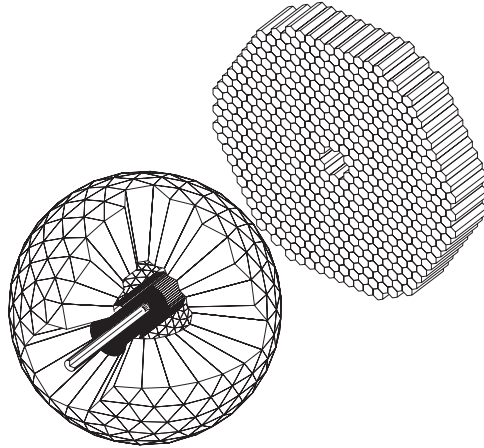


Figure 11: Crystal Ball detector with inner tracker and TAPS forward wall.

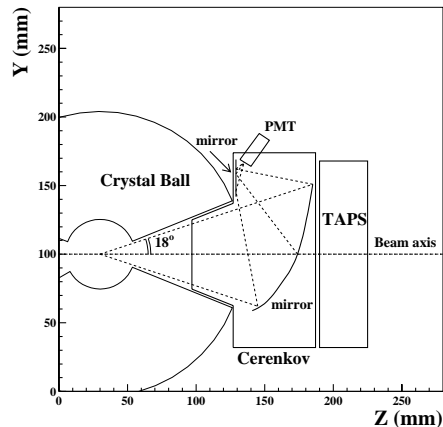


Figure 12: Schematic side view of the Crystal Ball with the Čerenkov detector.

zontal dilution refrigerator, presently under construction at Dubna, and a 5 T superconducting polarization magnet, which will be used in the polarization phase together with a microwave system for dynamical nuclear polarization (DNP). The polarization will be maintained during the measurement in the “frozen spin” mode at temperatures of about 50 mK by an internal

superconducting coil ( $B \simeq 0.4$  T) integrated into the dilution refrigerator. As target material we want to use butanol ( $C_4H_9OH$ ). At 2.5 T maximum proton polarization values close to 90% with a relaxation time in the "frozen spin" mode of about 200 hours can be expected. Based on our experience with the polarized Bonn target during the previous GDH experiments, the re-polarization phases will occur every second day for about 6 hours. The length of the target will be 2 cm ( $\phi \simeq 2.5$  cm) resulting in a total number of polarized protons of  $n_t = 0.8 \cdot 10^{23} \text{ cm}^{-2}$ , including the effects of dilution by unpolarizable nucleons and filling factor.

The photon induced reaction products will be registered by means of the Crystal Ball detector, complemented by the TAPS forward wall (see fig. 11) to increase the solid angle acceptance in forward direction, which is particularly important at higher energies (MAMI C). Together with the inner tracker detector consisting of two cylindrical multiwire proportional chambers and a thin cylindrical plastic scintillator barrel, a good charged particle identification is enabled.

In order to suppress electromagnetic background in forward direction on-line, we plan to use a threshold gas Čerenkov detector. Due to the spatial boundary conditions, it has to reach about 30 cm inside the Crystal Ball tunnel, see fig. 12. As Čerenkov medium the gas  $C_4F_{10}$  will be used which has a refractive index of  $n=1.0014$ . The threshold for electrons or positrons will be at 10 MeV, whereas the highest energy pions at MAMI C will be safely below threshold for Čerenkov radiation. The Čerenkov light is focussed via an ellipsoidal mirror on a small second mirror, which is needed to redirect the light onto the 5 inch photomultiplier tube. The large mirror has a 5cm diameter hole for the passage of the photon beam. The pieces of the previous Čerenkov detector from the GDH experiments can be reused, only the box has to be rebuilt, which will be done in Gent (Belgium).

While the use of the Čerenkov detector is absolutely necessary for total cross section measurements (see proposal [22] where also more details are included), it will also be very useful for differential cross section measurements of partial channels, since it will allow to increase the accessible angular range to smaller forward angles, where in general the strongest variations in cross sections and asymmetries are to be found.

The trigger conditions will be a combination of the standard cluster triggers requiring cluster multiplicities of 2 and  $\geq 3$ . The first condition is suitable for the 2 decay photons from  $\pi^0$  and  $\eta$  decays and will be scaled down, the second one for  $\pi^0\pi^0$  and  $\eta$  final states leading to 4 or 6 clusters.

### 3 Beam time estimate

The helicity asymmetry is determined from the measured asymmetry  $E_{meas}$  by

$$E = \frac{\eta}{P} E_{meas} = \frac{\eta}{P} \frac{N_P - N_A}{N_P + N_A},$$

where  $P$  is the product of the degrees beam and target polarizations,  $P = \overline{P}_\gamma \cdot \overline{P}_t$ , and  $\eta$  is the dilution factor, both from the butanol and from the other sources like target walls and helium.  $N_P$  and  $N_A$  are the total event numbers for parallel and anti-parallel spin configurations,

$$N_P = N_0(1 + PE + B + C)$$

$$N_A = N_0(1 - PE + B + C),$$

where  $N_0$  is the number of unpolarized events,  $B$  is the relative background contribution due to unpolarized target nucleons,  $C$  is the relative background contribution due to the target container and the helium.

The beam time required to reach a statistical accuracy of  $\delta E_{stat}$  is given by

$$\Delta t = \frac{\eta}{P^2} \cdot \frac{1}{\delta E_{stat}^2} [\dot{N}_\gamma \cdot n_t \cdot \varepsilon_{av} \cdot \overline{\sigma}_{unpol}]^{-1}$$

The parameters entering the count-rate estimate and resulting beam-time request are:

- Incoming electron beam energy:  $E_0 = 855$  MeV and 1500 MeV.
- Tagged photon energy range: upper 50% of the photon energy range.
- Average tagged photon flux over region of interest e.g. (800-1400 MeV):  
 $\dot{N}_\gamma = 3.6 \times 10^5 (s \cdot 20MeV)^{-1}$ .
- Number of polarized protons in a 2 cm long butanol target:  $n_t = 0.8 \times 10^{23} cm^{-2}$ .
- Total dilution factor:  $\eta = 1 + B + C = \frac{1}{f} + C = \frac{74}{10} + 4 = 11.4$ .  
 ( $\frac{1}{f}$  is the contribution of the target material butanol.)
- Beam and target polarizations:  $P = \bar{P}_\gamma \cdot \bar{P}_t = 0.6 \cdot 0.7 = 0.42$ .
- Average efficiency  $\varepsilon_{av} = 0.7$  (detection and reconstruction).
- Data acquisition capability: 1000 events/s (assuming an increase of a factor 2 compared to the existing readout due to a new S-Link electronics).

We aim at a statistical precision of  $\delta E_{stat} = 0.05$ , a bin size of 20 MeV in photon energy and of 10 bins in the angular distribution. The required beam time to reach this goal in the energy range 800-1400 MeV in case of single  $\pi^0$  production ( $\bar{\sigma}_{unpol} \approx 1.5\mu b/sr$ ) is 250 hours.

In order to improve the previous results in the  $D_{13}(1520)$  region and allow for some overlap, a second run with 855 MeV electron energy is necessary, which will also need 250 hours. Based on the experience with the previous GDH experiment, additional 150 hours will be required for target polarization, photon flux and Møller measurements. Data with a liquid hydrogen target will also be needed for unpolarized cross section data, but these can be measured in conjunction with other experiments.

This will result in high quality double polarization data for single and double  $\pi^0$  and  $\eta$  production. In the latter cases, where the cross sections are lower, the energy bin size will be increased to  $\Delta E_\gamma = \pm 20$  MeV and  $\delta E_{stat}$  will be somewhat increased. In addition, the charged pion production channels will also be included in the data set.

To summarize, the total beam time requested is:

**650 hours.**

## References

- [1] S.B. Gerasimov, *Sov. J. Nucl. Phys.* **2**, 430 (1966). S.D. Drell and A.C. Hearn, *Phys. Rev. Lett.* **16**, 908 (1966).
- [2] D. Drechsel *et al.*, *Nucl. Phys.* **A 645**, 145 (1999).
- [3] H. Dutz *et al.*, *Phys. Rev. Lett.* **94**, 162001 (2005).
- [4] J. Ahrens *et al.*, *Eur. Phys. J A* **21**, 323 (2004).
- [5] J. Ahrens *et al.*, *Phys. Rev. Lett.* **88**, 232002 (2002).
- [6] R.A. Arndt *et al.*, *Phys. Rev. C* **53**, 430 (1996), SAID (GWU) solution SM01.
- [7] D.E. Groom *et al.* *Eur. Phys. J. C* **15**, 1 (2000).
- [8] J. Ahrens *et al.*, *Eur. Phys. J A* **17**, 241 (2003).
- [9] W.-T. Chiang *et al.*, *Nucl. Phys. A* 700, 429-453 (2002).
- [10] A.V. Anisovich *et al.*, *Eur. Phys. J. A* **24**, 111 (2005).
- [11] J. Nacher *et al.*, *Nucl. Phys. A* **695**, 295 (2001); J. Nacher *et al.*, *Nucl. Phys. A* **697**, 372 (2002).
- [12] L. Murphy and J.-M. Laget, report DAPNIA-SPHN-95-42, 1995.
- [13] M. Hirata, N. Katagiri, T. Takaki, *Phys. Rev. C* **67**, 034601 (2003).
- [14] H. Holvoet, *PhD thesis*, University of Gent (2001).
- [15] W. Langgaertner *et al.*, *Phys. Rev. Lett.* **87**, 052001 (2001).
- [16] M. Effenberger *et al.*, *Phys. Rev.* **60**, 044614 (1999).
- [17] F. Klingl *et al.*, *Nucl. Phys. A* 624, 527 (1997).
- [18] J. Ahrens *et al.*, (GDH and A2 Collaborations), *Phys. Lett.* **551**, 49 (2003).
- [19] Assafiri *et al.*, *Phys. Rev. Lett.* 90, 222001 (2003).
- [20] F. Zapadtko, *PhD thesis*, J. Ahrens *et al.*, *Phys. Lett. B* (2005), (accepted).
- [21] A. Fix and H. Arenhövel, internal report MKPH-T-05-1.
- [22] P. Pedroni *et al.*, MAMI proposal (2005).